

AN ASTEROSEISMIC MEMBERSHIP STUDY OF THE RED GIANTS IN THREE OPEN CLUSTERS OBSERVED BY *Kepler*: NGC 6791, NGC 6819, AND NGC 6811

DENNIS STELLO,¹ SØREN MEIBOM,² RONALD L. GILLILAND,³ FRANK GRUNDAHL,⁴ SASKIA HEKKER,⁵ BENOÎT MOSSER,⁶
THOMAS KALLINGER,^{7,8} SAVITA MATHUR,⁹ RAFAEL A. GARCÍA,¹⁰ DANIEL HUBER,¹ SARBANI BASU,¹¹ TIMOTHY R. BEDDING,¹
KARSTEN BROGAARD,^{12,4} WILLIAM J. CHAPLIN,⁵ YVONNE P. ELSWORTH,⁵ JOANNA MOLENDĄ-ZAKOWICZ,¹³ ROBERT SZABÓ,¹⁴
MARTIN STILL,¹⁵ JON M. JENKINS,¹⁶ JØRGEN CHRISTENSEN-DALSGAARD,⁴ HANS KJELDSSEN,⁴ ALDO M. SERENELLI,¹⁷
BILL WOHLER,¹⁸

Draft version September 25, 2018

ABSTRACT

Studying star clusters offers significant advances in stellar astrophysics due to the combined power of having many stars with essentially the same distance, age, and initial composition. This makes clusters excellent test benches for verification of stellar evolution theory. To fully exploit this potential, it is vital that the star sample is uncontaminated by stars that are not members of the cluster. Techniques for determining cluster membership therefore play a key role in the investigation of clusters. We present results on three clusters in the *Kepler* field of view based on a newly established technique that uses asteroseismology to identify fore- or background stars in the field, which demonstrates advantages over classical methods such as kinematic and photometry measurements. Four previously identified seismic non-members in NGC 6819 are confirmed in this study, and three additional non-members are found – two in NGC 6819 and one in NGC 6791. We further highlight which stars are, or might be, affected by blending, which needs to be taken into account when analysing these *Kepler* data.

Subject headings: stars: fundamental parameters — stars: oscillations — stars: interiors — techniques: photometric — open clusters and associations: individual (NGC 6791, NGC 6819, NGC 6811)

1. INTRODUCTION

Determination of cluster membership is a crucial step in the analysis of stellar clusters. Stars in an open cluster are thought to have formed from the same interstellar cloud of gas and

dust, and hence share a common age and space velocity. Cluster membership can therefore be inferred from the location of the stars along an isochrone in the color-magnitude diagram (photometric membership), and from their common space velocity (kinematic membership) measured as the line-of-sight radial velocity and the perpendicular proper motion. Recently, a new independent method was introduced by Stello et al. (2010) who performed an asteroseismic analysis based on the first month of data from the *Kepler Mission* (Koch et al. 2010) to infer the cluster membership for a small sample of red giant stars in NGC 6819. Asteroseismology has the advantage that the oscillations in a star, which depend on the physical properties of the star’s interior (Christensen-Dalsgaard 2004), are independent of stellar distance, interstellar extinction, and any random alignment between the space velocity of the cluster and field stars. In particular, the so-called average large frequency separation, $\Delta\nu$, between consecutive overtone oscillation modes depends on the mean density of the star, and the frequency of maximum oscillation power, ν_{\max} , is related to its surface gravity and effective temperature. Both $\Delta\nu$ and ν_{\max} are known to scale with the basic stellar properties, M , L , and T_{eff} , (Ulrich 1986; Kjeldsen & Bedding 1995) and can therefore be used to infer those properties without relying on detailed modelling of stellar interiors (e.g. Stello et al. 2008; Kallinger et al. 2010b).

We now have *Kepler* time series photometry that span 10 times longer than in the work by Stello et al. (2010). In this paper we are therefore able to present an asteroseismic membership analysis of a more comprehensive set of red giant stars in three open clusters within *Kepler*’s fixed field of view: NGC 6791, NGC 6819, and NGC 6811. We are further able to measure and make use of both $\Delta\nu$ and ν_{\max} for this purpose. In addition, to facilitate our inference on cluster membership and obtain more robust results we include an investigation of T_{eff} found from different color indices and present a detailed

¹ Sydney Institute for Astronomy (SIFA), School of Physics, University of Sydney, NSW 2006, Australia

² Harvard-Smithsonian Center for Astrophysics, 60 Garden Street, Cambridge, MA, 02138, USA

³ Space Telescope Science Institute, 3700 San Martin Drive, Baltimore, Maryland 21218, USA

⁴ Department of Physics and Astronomy, Aarhus University, Ny Munkegade 120, 8000 Aarhus C, Denmark

⁵ School of Physics and Astronomy, University of Birmingham, Edgbaston, Birmingham B15 2TT, UK

⁶ LESIA, CNRS, Université Pierre et Marie Curie, Université Denis Diderot, Observatoire de Paris, 92195 Meudon, France

⁷ Institute for Astronomy, University of Vienna, Türkenschanzstrasse 17, 1180 Vienna, Austria

⁸ Department of Physics and Astronomy, University of British Columbia, 6224 Agricultural Road, Vancouver, BC V6T 1Z1, Canada

⁹ High Altitude Observatory, NCAR, P.O. Box 3000, Boulder, CO 80307, USA

¹⁰ Laboratoire AIM, CEA/DSM-CNRS, Université Paris 7 Diderot, IRFU/SaP, Centre de Saclay, 91191, Gif-sur-Yvette, France

¹¹ Department of Astronomy, Yale University, P.O. Box 208101, New Haven, CT 06520-8101

¹² Department of Physics & Astronomy, University of Victoria, P.O. Box 3055, Victoria, B.C., V8W 3P6, Canada

¹³ Instytut Astronomiczny Uniwersytetu Wrocławskiego, ul. Kopernika 11, 51-622 Wrocław, Poland

¹⁴ Konkoly Observatory of the Hungarian Academy of Sciences, Konkoly Thege Miklós út 15-17, H-1121 Budapest, Hungary

¹⁵ Bay Area Environmental Research Institute/NASA Ames Research Center, Moffett Field, CA 94035, USA

¹⁶ SETI Institute/NASA Ames Research Center, MS 244-30, Moffat Field, CA 94035, USA

¹⁷ Instituto de Ciencias del Espacio (CSIC-IEEC), Facultad de Ciències, Campus UAB, 08193 Bellaterra, Spain

¹⁸ Orbital Sciences Corporation/NASA Ames Research Center, Moffett Field, CA 94035

analysis of blending. Our membership results are compared with those from classical techniques.

We refer to our four companion papers for additional asteroseismic exploration of the same cluster data including (i) the determination of stellar mass and radius and cluster distances (Basu et al. 2011), (ii) verification of scaling relations for $\Delta\nu$ and ν_{\max} (Hekker et al. 2011), (iii) derivation of a new scaling relation for oscillation amplitude (Stello et al. 2011), (iv) and mass loss properties of red giants during their transition between the hydrogen-shell and core-helium-burning phases (Miglio et al. 2011). Like this paper, these studies are based on the global asteroseismic seismic properties, $\Delta\nu$, ν_{\max} and amplitude, while more detailed frequency analyses requires more data for these relative faint and crowded cluster stars.

2. TARGET SELECTION

For the purpose of determining cluster membership we use only stars showing oscillations that are stochastically driven by near-surface convection (solar-like oscillations) because their seismic observables are strongly linked to the fundamental stellar properties described by well established scaling relations (see Sect. 6). This limits our current study to the red giants as we require the oscillations to be sufficiently sampled by the spacecraft’s half-hour cadence.

Large 200-pixel ‘super’ stamps of the CCD images (13’3 on the side) centered on NGC 6791 and NGC 6819 are obtained at a half-hour cadence throughout the mission, eventually providing photometric time series (light curves) of all resolved stars within them (Figure 1). However, these stamps require special image processing, which is still pending. We therefore base our current study on our initial selection of individual cluster stars made prior to launch, which have followed the standard *Kepler* data reduction of the raw images (Sect. 3), and includes a few stars outside the super stamps. Due to general limits on the number of stars that can be recorded by *Kepler* at any given time, the selection was aimed at maximising the number of cluster members in our sample.

For NGC 6791 no comprehensive kinematic membership study was available so the selection was based on photometric membership which we determined using the photometry by Stetson et al. (2003). Only stars quite close to the empirical isochrone in the color-magnitude diagram were chosen (Figure 2, large dots). We note that with this strict selection criterion we risk missing genuine members that are further away from the main cluster sequence, and hence might not sample the full intrinsic scatter of the population. Our selection provided 101 red giant stars.

We selected 63 red giants in the open cluster NGC 6819 that had more than 80% membership probability from the radial velocity survey of Hole et al. (2009). Being purely kinematic, this selection is more likely to include stars that do not follow the standard single-star evolution. Indeed, Figure 2 shows that a number of stars marked as kinematic members (large dots) are quite far from the empirical isochrone formed by the majority of stars.

In the case of NGC 6811 we chose all stars determined to be possible members from a preliminary radial velocity survey (Meibom) (Figure 2), which gave us five red giants in total.

For this purpose the data are obtained in the spacecraft’s long-cadence mode .

3. OBSERVATIONS AND DATA REDUCTION

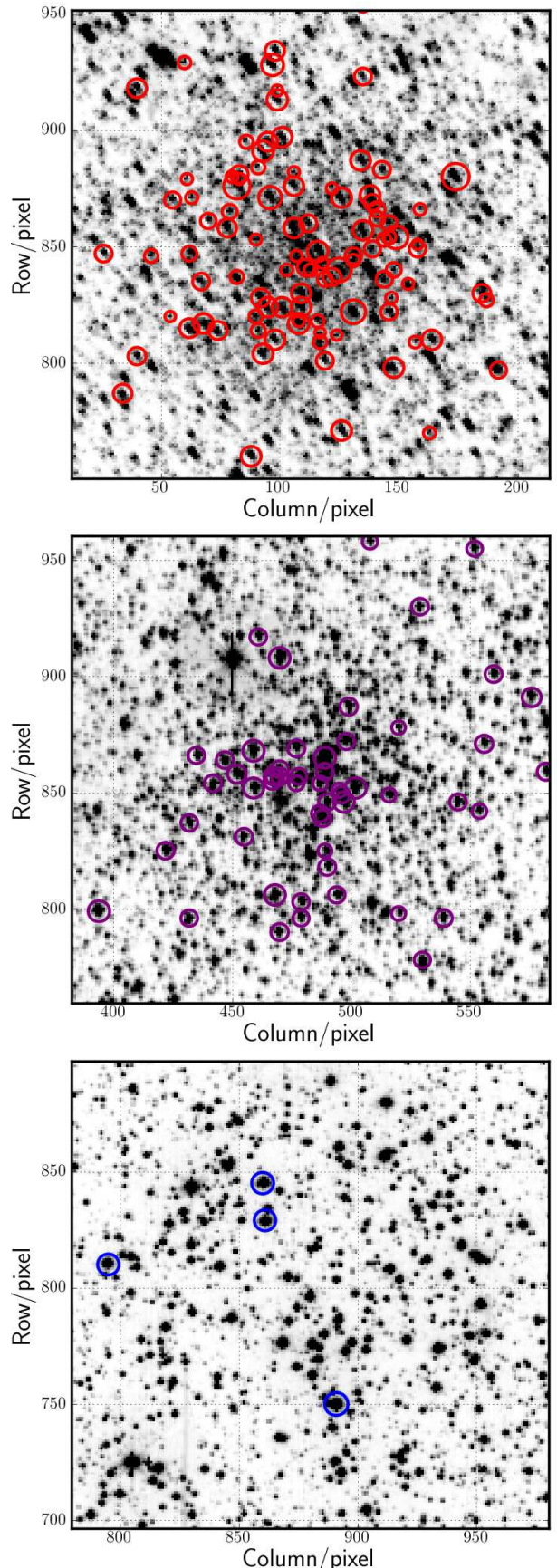


FIG. 1.— Cluster super stamps of NGC 6791 (top) and NGC 6819 (middle). A similar size stamp is shown for NGC 6811 (bottom) to illustrate the difference in crowding. A total of 99 (NGC 6791), 54 (NGC 6819), and 4 (NGC 6811) of the pre-launch selected targets fall within these stamps (encircled).

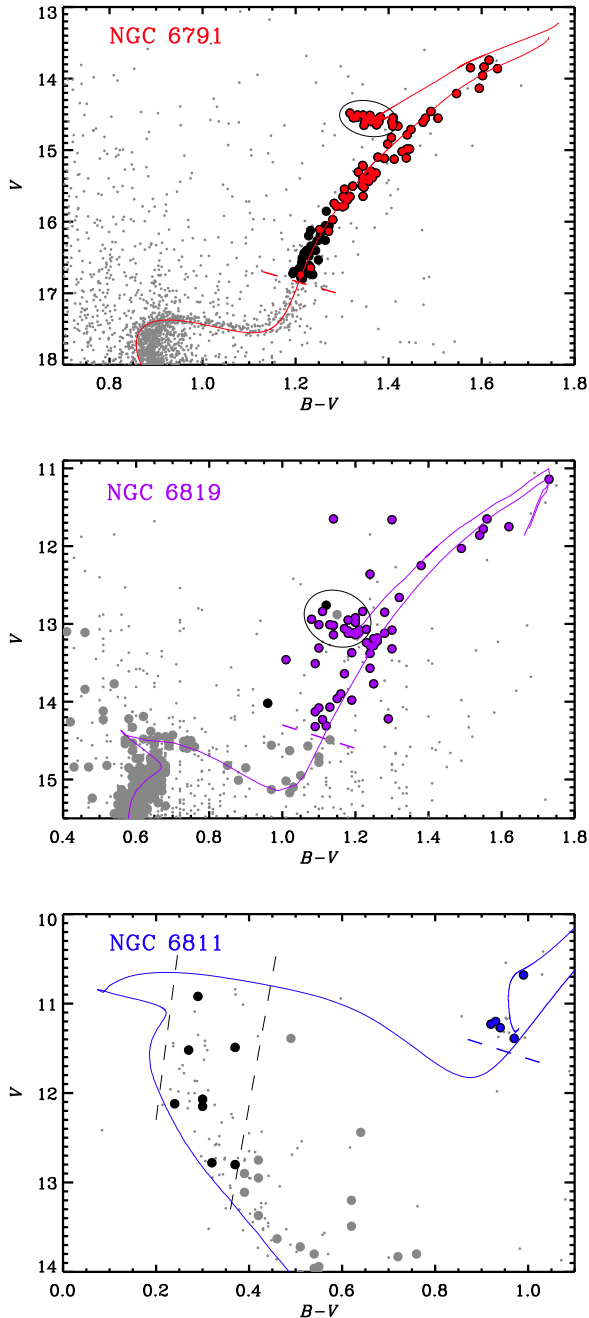


FIG. 2.— Color-magnitude diagrams of the clusters. Photometry is from Stetson et al. (2003) (NGC 6791), Hole et al. (2009) (NGC 6819), and the Webda database (<http://www.univie.ac.at/webda/>) (NGC 6811). Representative isochrones from Pietrinferni et al. (2004) (NGC 6791 and NGC 6811) and Marigo et al. (2008) (NGC 6819) are matched to the red giant stars to guide the eye. Near horizontal dashed lines mark the sampling limit for solar-like oscillations with *Kepler*'s long-cadence mode. Large black dots show stars for which *Kepler* data are currently available, while large colored dots (red, purple and blue) indicate the subset of these which show evidence of solar-like oscillations. All large dots in the two lower panels show likely members from radial velocity surveys (Hole et al. 2009 and unpublished work by Meibom). Vertical dashed lines mark the approximate location of the classical instability strip. Stars marked as ‘Clump star’ in Tables 1 and 2 are encircled.

The photometric time series data presented here were obtained in ‘long cadence’ ($\Delta t \sim 30$ min, Jenkins et al. (2010a)) between 2009 May 12 and 2010 March 20, known as observing quarters 1–4 (Q1–Q4). Within this period the spacecraft’s long-cadence mode provided approximately 14,000 data points per star. The raw images were processed by the standard *Kepler* Science Pipeline and included steps to remove signatures in the data from sources such as pointing drifts, focus changes, and thermal variations all performed during the Pre-search Data Conditioning (PDC) procedure (Jenkins et al. 2010b). PDC also corrects for flux from neighboring stars within each photometric aperture based on a static aperture model. However, this model is not adequate for all stars, due to small changes in the telescope point-spread-function and pointing between subsequent quarterly rolls when the spacecraft is rotated 90 degrees to align its solar panels. As a result the light curves show jumps in the average flux level from one quarter to the next. To correct for that we shifted the average flux levels for each quarter to match that of the raw (pre-PDC) data before stitching together the time series from all four quarters. This ensured that the relative flux variations were consistent from one quarter to the next. We compared our corrected (post-PDC) data with the raw data and also after we performed a number of ‘manual’ corrections based entirely on the appearance of the light curves (hence not taking auxiliary house-keeping data such as pointing into account). These corrections included removal of outliers, jumps, and slow trends in a similar way as the approach by Garcia et al. (2011). The comparison revealed that for a few stars PDC did not perform well, in which case we chose the raw or ‘manually’ corrected raw data.

4. BLENDING AND LIGHT CURVE VERIFICATION

The super stamps in Figure 1 clearly illustrate that blending is an issue we need to address before proceeding with the analysis of these cluster data. Some stars show clear signatures of blending arising from the relatively large pixel scale ($\sim 4''$) of the *Kepler* photometer compared to the fairly crowded cluster fields. Blending will give rise to additional light in the photometric aperture, which will reduce the relative stellar variability, and increase the photon counting noise. In severe cases, the detected stellar variability arises from a blending star and not the target.

We have studied the effects from blending by looking at correlations between light curves of all the target stars (black, red, purple, and blue dots in Figure 2). The light curve correlations show no significant increase unless the stars are within approximately five pixels of each other and the blending star is at least as bright as the target (Figure 3). We visually assessed the light curves of all stars separated by less than five pixels, and identified those that showed clear correlation over extended periods of time as blends. We list the blending stars in Table 1 (column-3), Table 2 (column-4), and Table 3 (column-4). Also listed here, is the variability type of blending stars identified from single light curves that clearly showed variability from two stars. If the variability included the expected seismic signal of the target, under the assumption that the target was a cluster member, we interpreted the additional signal as caused by a blend. We see no blending for our NGC 6811 targets. We note that the stars for which we currently have light curves are far from all stars in the vicinity of the clusters (see Figure 1). It is therefore likely that our correlation analysis has not revealed all blends. For the two most crowded clusters (NGC 6791 and NGC 6819) there are

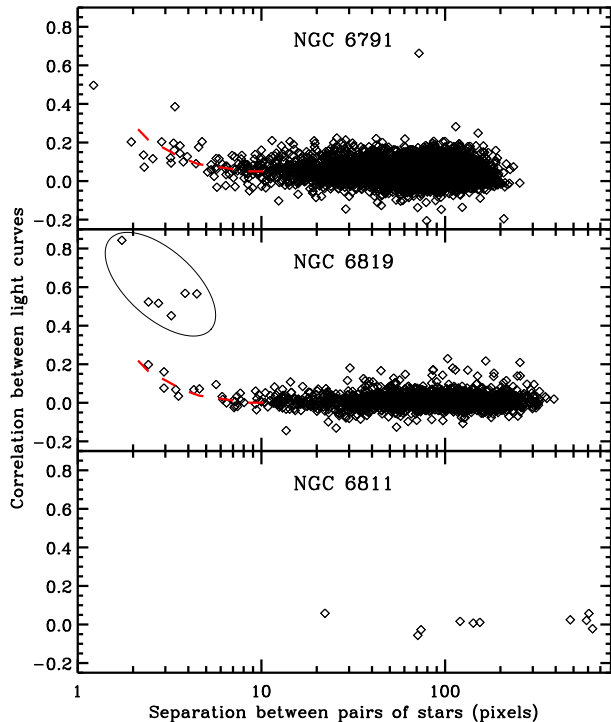


FIG. 3.— Correlation coefficients for light curves of all pairs of stars in our target list shown as a function of their separation on the CCD. Fiducial dashed line indicates the average increase in correlation towards lower separations. There is one pair of stars in NGC 6791 that show large correlation despite their large separation (see text). The six pairs of stars with abnormally high correlation coefficients in NGC 6819 are all blended by the W UMa variable KIC5112741 (see text).

about 1000 stars brighter than $Kp \simeq 16.5$ within the super stamps. We expect a significant fraction of those stars to be accessible when these stamps have been analyzed, which will further aid the characterisation of blending.

In addition to the light curve correlations, we identified all significantly bright stars nearby each target using information from the *Kepler Input Catalogue* (KIC), which was designed to reach down to $Kp \lesssim 16.0$. This was just adequate for our purpose. We identified targets to be potentially affected by blending if there were stars within five pixels that were at least half as bright as the target itself, which we regard a conservative choice given the results from the above correlation analysis. Potentially blended targets are listed in Table 1 (column-4), Table 2 (column-5), and Table 3 (column-5), while the blending stars, their flux ratios with respect to the target, and their separations are given in Tables 4 and 5. Again, the NGC 6811 targets show no signs of potential blending. Due to slight temporal changes in telescope pointing, the degree of blending for each target can vary considerably over time for the crowded cluster fields. We took this into account in our approach to correct the light curves, which we describe in detail below for the two clusters affected by blending and other possibly related effects.

4.1. NGC 6791

There is one pair of stars (KIC2569488, 2568916) that show an abnormally high correlation despite their large separation (~ 70 pixels) (see Figure 3). Visual inspection of the light curves reveals that it arises from a strong trend localized

within a relatively narrow time span. They are not mutually influenced by a bad column, neither do they lie within the wings of a really bright star. From inspection of the raw images they should not correlate, and there are no indications that the oscillation signals of the two are affected by each other. We therefore leave the light curves uncorrected.

The Q1 data were not used for KIC2570384, and Q3 was not used for KIC2437488, both due to apparent blending by short-period eclipsing binaries. Possible candidates for these blends can be found in Table 4 (column-2). An abnormally strong peak of unknown origin was seen slightly offset from the main excess envelope in the power spectrum of KIC2569935. Hence, to avoid strong bias in the measurement of the asteroseismic parameters, we fitted and removed a corresponding single sine wave from the data.

4.2. NGC 6819

The four stars KIC5024582, 5112734, 5112751, and 5112741 form six correlation pairs that stand out in Figure 3 (encircled). It turns out that the increased correlation is caused by the same large-amplitude contact binary (W UMa variable), KIC5112741. Fortunately, we were able to retrieve the pulsation signal to a degree that allowed the measurement of the seismic parameters used in this paper (see Sect. 5) except for the W UMa variable itself. We did that by applying a high-pass filter to the three affected light curves using a moving average of two days. The resulting light curves show correlation coefficients in line with the trend shown by the dashed line in Figure 3. We followed the same approach to remove the variability of what appears to be a bright M-giant (most likely KIC5024470, Table 5 column-2), from the light curve of KIC5024456, in this case using a four-day moving average.

The Q1 data were not used for KIC5024583 due to the presence of an eclipsing binary signal. KIC5024268 was also significantly affected by apparent blending by a δ Scuti star in the Q1 and Q2 data. These data were therefore removed from the light curve. Like in one of the NGC 6791 targets, KIC4937770 showed an abnormal peak in the power spectrum, which we removed by fitting a single sine wave.

5. EXTRACTION OF ASTEROSEISMIC PARAMETERS

In Figure 4 we show a typical example of a power spectrum and indicate for illustration the average large separation, $\Delta\nu$, and the frequency of maximum oscillation power, ν_{\max} . Values of $\Delta\nu$ and ν_{\max} were extracted from the data using each of the time series analysis pipelines described in Hekker et al. (2010); Huber et al. (2009); Kallinger et al. (2010a); Mathur et al. (2010); Mosser & Appourchaux (2009). If at least one pipeline detected oscillations, the star was included in our sample for further investigation. The results of all stars were then verified by visual inspection of the power spectrum and the autocorrelation of the power spectrum. We further verified values of $\Delta\nu$ by forming the so-called échelle diagram of the power spectrum, constructed by dividing the power spectrum into segments, each $\Delta\nu$ wide, which were then stacked one above the other. To illustrate, Figure 5 shows three examples of the échelle diagram for the same star, each based on a slightly different segment width (adopted large separation). If $\Delta\nu$ is correct, the radial oscillation modes form a vertical ridge in the échelle, offset from zero by ϵ in agreement with recent results on the ϵ - $\Delta\nu$ relation of red giants (Huber et al. 2010; Mosser et al. 2011; White et al. 2011). The échelle diagram clearly reveals if the adopted large separation is too small (ridges tilt to the right; panel A) or too

TABLE 1
TARGET PROPERTIES OF NGC 6791.

Target ID ^a (KIC) [1]	Target ID (Stetson) ^b [2]	Blend known [3]	Blend potential [4]	Clump star [5]	Membership (M&P) ^c [6]	Membership (Garnavich) ^d [7]	Member (Other) ^e [8]	Seismic member [8]
2297384	5583	No	Yes	Yes				Yes
2297793	11539	No	No	No		R18/No?		No
2297825	11957	No	No	Yes				Yes
2435987	611	No	Yes	No				Yes
2436097	1110	No	No	No				Yes
2436209	1705	No	No	No				Yes
2436332	2309	No	Yes	No	33%			Yes
2436417	2723	No	No	Yes	17%		W	Yes
2436458	2915	No	Yes	No	49%			Yes
2436540	3354	No	No	No				Yes
2436593	3609	No	Yes	No	13%			Yes
2436676	4122	No	No	No	88%			Yes
2436688	4202	No	Yes	No	98%			Yes
2436732	4482	No	No	Yes	98%			Yes
2436759	4616	No	Yes	No	88%			Yes
2436814	4952	No	Yes	No			W	Yes
2436818	4968	No	No	No				Yes
2436824	4994	No	Yes	No	82%			Yes
2436900	5454	No	Yes	No	98%			Yes
2436912	5503	No	Yes	Yes	88%			Yes
2436944	5712	No	No	Yes	23%			Yes
2436954	5787	2436944	Yes	No				Yes
2437040	6288	No	Yes	No	29%			Yes
2437103	6626	No	Yes	No				Yes
2437171	6963	2437209	Yes	No	98%	R4/Yes	O	?
2437240	7347	No	Yes	No	99%			Yes
2437270	7564	No	Yes	No	89%			Yes
2437325	7912	No	Yes	No	97%			Yes
2437340	7972	No	No	No	92%	R19/Yes	C	Yes
2437353	8082	No	Yes	Yes	93%		C,Gr	Yes
2437394	8317	No	Yes	No	98%			Yes
2437402	8351	No	Yes	No	96%			Yes
2437444	8563	No	No	No			C	Yes
2437488	8865	Binary*	Yes	No				Yes
2437496	8904	No	Yes	No	42%	R12/Yes	O	Yes
2437507	8988	No	No	No	29%		C	Yes
2437564	9316	No	Yes	Yes	24%		Gr	Yes
2437589	9462	No	No	Yes	99%			Yes
2437653	9827	No	Yes	No	94%			Yes
2437698	10135	No	No	Yes	77%			Yes
2437781	10674	No	Yes	No				Yes
2437804	10809	No	Yes	Yes	97%			Yes
2437805	10806	No	Yes	Yes	97%		Gr	Yes
2437816	10898	No	No	No	68%		C	Yes
2437851	11116	No	Yes	No	17%			?
2437933	11598	No	Yes	No	94%			Yes
2437957	11797	No	Yes	No	11%			Yes
2437965	11814	No	Yes	No	98%	R8/Yes	C	Yes
2437972	11862	No	Yes	No	85%			Yes
2437976	11895	No	Yes	No	98%			Yes
2437987	11938	No	Yes	Yes	96%			Yes
2438038	12249	No	Yes	No	96%			Yes
2438051	12333	No	Yes	Yes	99%			Yes
2438140	12836	No	No	No				Yes
2438333	13847	No	No	No				Yes
2438421	14379	No	No	No	47%	R7/Yes	O	?
2568916	996	No	No	Yes				Yes
2569055	1904	No	No	Yes				Yes
2569360	3754	No	No	No	94%		W	Yes
2569488	4715	No	No	Yes	49%		C	Yes
2569618	5796	No	No	No	99%			Yes
2569935	8266	High peak*	No	No		R16/Yes	O,C	Yes
2569945	8395	No	Yes	Yes	89%			Yes
2570094	9786	No	Yes	No	85%			Yes
2570172	10407	No	Yes	No				Yes
2570214	10695	No	Yes	Yes	88%			Yes
2570244	11006	No	Yes	No	90%			Yes
2570384	12265	Binary*	Yes	No				Yes
2570518	13260	No	Yes	No				Yes

^aOnly targets for which we detect oscillations are listed.^bIDs from Stetson et al. (2003).^cPreliminary membership probabilities from radial velocity (Meibom &

TABLE 2
TARGET PROPERTIES OF NGC 6819.

Target ID ^a (KIC) [1]	Target ID (Hole et al.) ^b [2]	Target ID (Sanders) ^c [3]	Blend known [4]	Blend potential [5]	Clump star [6]	Class. (Hole et al.) ^b [7]	Membership (Hole et al.) ^b [8]	Membership (Sanders) ^c [9]	Photometric member [10]	Seismic member [11]
4936335	007021	9	No	No	No	SM	95%	68%	Yes	No
4937011	007017	90	No	No	No	SM	95%	90%	Yes	No
4937056	002012	103	No	No	Yes	BM	95%	92%	Yes	Yes
4937257	009015	144	No	No	No	SM	88%	80%	No	No
4937576	005016	173	No	No	No	SM	91%	88%	Yes	Yes
4937770	009024		High peak*	No	No	SM	94%		No	Yes
4937775	009026		No	No	No	BM	91%		No	Yes
5023732	005014	27	No	No	No	SM	94%	90%	Yes	Yes
5023845	008010	36	No	No	No	SM	95%	89%	Yes	Yes
5023889	004014	42	No	No	No	U	95%	90%	No	No
5023931	007009	43	No	No	No	BM	84%	91%	Yes	Yes
5023953	003011	45	No	No	Yes	BLM		90%	Yes	Yes
5024043	008013	58	No	No	Yes	SM	95%	65%	Yes	Yes
5024143	007005	65	No	No	No	SM	94%	69%	Yes	Yes
5024240	008007		No	No	No	BM	88%		Yes	Yes
5024268	002003	78	δ Scuti*	No	No	SM	93%	92%	No	No
5024272	003003	79	No	No	No	SM	95%		No	No
5024297	008003	87	5024312	Yes	No	SM	89%	92%	Yes	Yes
5024312	013002	86	5024297	Yes	No	SM	89%	87%	Yes	Yes
5024327	011002	96	No	No	Yes	SM	94%	88%	Yes	Yes
5024404	003004	98	No	No	No	SM	93%	81%	Yes	Yes
5024405	004001	100	No	Yes	No	SM	93%	91%	Yes	Yes
5024414	006002	106	No	Yes	Yes	SM	95%	91%	Yes	?
5024456	001002	110	M-giant*	Yes	No	SM	88%	72%	Yes	Yes
5024476	001006	111	No	No	Yes	BLM		89%	Yes	?
5024512	003001	116	No	Yes	No	SM	93%	90%	Yes	Yes
5024517	002001		No	Yes	No	SM	88%		Yes	?
5024582	009002	118	5112741*	Yes	Yes	BLM		87%	Yes	Yes
			5024601							
5024583	007003	119	Binary*	Yes	No	SM	95%	92%	Yes	Yes
5024601	004002	124	5024582	Yes	Yes	SM	92%	86%	Yes	Yes
5024750	001004	141	No	No	No	SM	93%	83%	Yes	Yes
5024851	002008	152	No	No	No	BLM		64%	Yes	Yes
5024967	006009	158	No	No	Yes	SM	92%	87%	Yes	Yes
5111718	008018	10	No	No	No	SM	95%	91%	Yes	Yes
5111940	005012	28	No	Yes	No	SM	94%	79%	Yes	Yes
5111949	004011	30	No	No	Yes	SM	93%	83%	Yes	Yes
5112072	009010	39	No	No	No	SM	95%	91%	Yes	Yes
5112288	002007	64	No	No	Yes	SM	93%	90%	Yes	Yes
5112361	004008	70	No	No	No	BM	91%	78%	No	Yes
5112373	005005	74	No	No	Yes	SM	95%	87%	Yes	Yes
5112387	003007	73	No	No	Yes	SM	95%	88%	Yes	Yes
5112401	003009	75	No	No	Yes	SM	95%	92%	Yes	Yes
5112403	005004	77	No	No	No	SM	91%	89%	Yes	Yes
5112467	006003	85	No	Yes	Yes	SM	95%	87%	Yes	Yes
5112481	001007	93	No	No	No	SM	92%	89%	Yes	Yes
5112491	010002	89	No	Yes	Yes	SM	95%	92%	Yes	Yes
5112730	004005	128	No	No	Yes	SM	93%	62%	Yes	Yes
5112734	012002	130	5112741*	Yes	No	SM	91%	90%	Yes	Yes
5112744	005011	127	No	No	No	SM	95%	77%	Yes	Yes
5112751	008002	131	5112741*	Yes	Yes	SM	93%	89%	Yes	?
5112786	005003	134	No	No	No	SM	94%	69%	Yes	Yes
5112880	002004	145	No	No	No	SM	81%	1%	Yes	Yes
5112938	002006	150	No	Yes	Yes	SM	89%	88%	Yes	Yes
5112948	005007	147	No	No	No	SM	93%	89%	Yes	Yes
5112950	003005	148	No	No	Yes	SM	95%	92%	Yes	Yes
5112974	004009	151	No	No	Yes	SM	94%	91%	Yes	Yes
5113041	004007	153	No	No	No	SM	94%	26%	Yes	Yes
5113061	001014	157	No	No	No	SM	95%	89%	Yes	Yes
5113441	012016	185	No	No	No	SM	89%	0%	Yes	Yes
5199859	001016	69	No	No	No	SM	95%	89%	Yes	Yes
5200152	003021		No	No	Yes	SM	94%		Yes	Yes

^aOnly targets for which we detect oscillations are listed.

^bID, classification, and membership probability from radial velocity (Hole et al. 2009); SM: single member; BM: binary member; BLM: binary likely member; U: Unknown.

^cID and membership probability from proper motion (Sanders 1972).

*Signal removed from light curve.

TABLE 3
TARGET PROPERTIES OF NGC 6811.

Target ID ^a (KIC) [1]	Target ID (Sanders) ^b [2]	Target ID (Dias et al.) ^c [3]	Blend known [4]	Blend potential [5]	Clump star [6]	Class. (M&M) ^d [7]	Membership (Meibom) ^e [8]	Membership (Sanders) ^b [9]	Membership (Dias et al.) ^c [10]	Photometric member [11]	Seismic member [12]
9534041			No	No	Yes		SLM 74%			Yes	Yes
9655101	95	TYC3556-00530-1	No	No	Yes	SM	SM 84%	97%	95%	Yes	Yes
9655167	106		No	No	Yes	BM	BLM 57%	97%		Yes	Yes
9716090	92	TYC3556-02356-1	No	No	Yes	SM	SM 78%	94%	95%	Yes	Yes
9716522	170	TYC3556-02634-1	No	No	Yes*	SM	SM 79%	97%	97%	Yes	Yes

^aOnly targets for which we detect oscillations are listed.

^bID and membership probability from proper motion (Sanders 1971).

^cTycho ID and membership probability from proper motion (Dias et al. 2002).

^dClassification from radial velocity measurements (Mermilliod & Mayor 1990); SM: single member; BM: binary member.

^eClassification and membership probability from radial velocity measurements (Meibom); SLM: single likely member; BLM: binary likely member.

*Star appears to be towards the end of He-core burning (Figure 2).

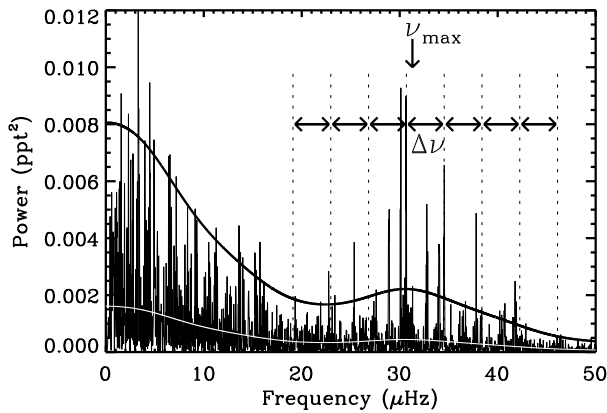


FIG. 4.— Power spectrum of KIC2436824. The average large frequency separation, $\Delta\nu$, and the frequency of maximum power, ν_{\max} , are indicated with arrows. The equally spaced dashed lines have been positioned to coincide with the radial mode near ν_{\max} . The solid white curve shows the spectrum convolved with a Gaussian function of FWHM = $4\Delta\nu$, which we also show after multiplying by five for clarity (thick black curve).

large (ridges tilt to the left; panel C) even by a few percent. For almost all stars multiple pipelines returned results, and in the vast majority of cases the results agreed within a few percent. With such small scatter our conclusions about membership would essentially be independent on our choice of the final set of results. We therefore adopted the results from the pipeline that returned results for most stars, except for the few stars where $\Delta\nu$ was clearly wrong (échelle ridges strongly tilted), in which case we chose the pipeline results that generated the most vertical ridges in the échelle. We were able to detect oscillations in all the red giants in our sample except two stars in NGC 6819 (KIC5112741 and 5200787) and towards the faint end of stars in NGC 6791 ($15.8 < V < 16.8$, $15.5 < Kp < 16.5$), for which higher signal-to-noise data, hence longer light curves, will be required.

For some of the most luminous stars, which oscillate at very low frequencies, $\Delta\nu$ is quite small and was difficult to determine reliably with the length of our current dataset. The dominant periodicity, P_{\max} , equivalent to $1/\nu_{\max}$, was however

easily detectable in the Fourier spectrum and even directly in the time series (Figure 6). The uncertainty in ν_{\max} for these stars is relatively large because it was not always possible to correct for the background granulation signal.

6. MEMBERSHIP

Following the approach by Stello et al. (2010), we will use asteroseismic measurements to categorise our selected stars into asteroseismic cluster members or likely non-members. We note that the length of the data analysed by Stello et al. (2010) only allowed robust measurement of ν_{\max} for many of their targets. With our current data we can also extract $\Delta\nu$ for almost all the target stars, which is generally the more precise measurement of the two. The former parameter is known to scale with acoustic cut-off frequency, and hence (Brown et al. 1991; Kjeldsen & Bedding 1995; Mosser et al. 2010):

$$\nu_{\max} \simeq \frac{M/M_{\odot} (T_{\text{eff}}/T_{\text{eff},\odot})^{3.5}}{L/L_{\odot}} \nu_{\max,\odot}, \quad (1)$$

where $T_{\text{eff},\odot} = 5777$ K and $\nu_{\max,\odot} = 3100$ μHz , while the latter scales with the square root of the mean density of the star (Ulrich 1986; Kjeldsen & Bedding 1995):

$$\Delta\nu \simeq \frac{(M/M_{\odot})^{0.5} (T_{\text{eff}}/T_{\text{eff},\odot})^3}{(L/L_{\odot})^{0.75}} \Delta\nu_{\odot}, \quad (2)$$

where $\Delta\nu_{\odot} = 135$ μHz .

Because M and T_{eff} vary only slightly compared to L within a sample of cluster red giants, a tight correlation is expected between both $\Delta\nu$ or ν_{\max} and the apparent stellar magnitude, which for cluster members is indicative of luminosity. By plotting stellar apparent magnitude versus $\Delta\nu$ or ν_{\max} we indeed see a tight correlation apart from a few outliers. To illustrate, we show 2MASS K magnitude (Skrutskie et al. 2006) versus $\Delta\nu$ in Figure 7 (panel A). We note that there is no apparent correlation between the crowding value from *KIC* and whether stars follow the expected correlation or not. This suggests that the *KIC* crowding value is not a robust indicator of how much $\Delta\nu$ and ν_{\max} are affected by blending. This is expected because increased blending does not alter the oscillation frequencies of the target but only adds extra noise and lowers the relative amplitude of the oscillations. Only in the rare event where the oscillation signal from

TABLE 4
POTENTIAL BLENDS FOR NGC 6791 TARGETS.

Target ID ^a (KIC)	Blend (KIC)	$\frac{\text{Flux}_B}{\text{Flux}_T}$ ^b	Sep (pix)	Target ID ^a (KIC)	Blend (KIC)	$\frac{\text{Flux}_B}{\text{Flux}_T}$ ^b	Sep (pix)
2297384	2297357	6.94	5.0	2437564	2437593	0.51	1.7
2435987	2435967	0.51	4.1	2437653	2437672	0.99	1.0
2436332	2436354	2.18	3.3		2437641	0.67	3.2
2436458	2436455	0.53	4.8		2437648	5.61	2.7
2436593	2436608	2.41	1.6		2437693	3.88	3.1
2436688	2436641	0.79	4.3		2437706	0.79	4.1
2436759	2436750	4.28	1.0	2437781	2437775	4.24	0.8
	2436746	0.51	1.0	2437804	2437803	0.69	0.8
2436814	2436879	0.85	4.8		2437871	0.91	4.8
	2436826	1.30	0.7	2437805	2437747	0.51	4.3
2436824	2436848	0.50	2.2	2437851	2437816	8.90	3.8
2436900	2436911	0.51	1.7		2437797	0.58	4.2
2436912	2436881	0.63	2.8	2437933	2437931	1.46	4.8
	2436879	0.83	3.3		2437928	0.55	4.4
	2436897	1.52	1.4		2437957	1.18	4.6
	2436866	2.74	2.9	2437957	2437933	0.85	4.6
2436954	2569626	0.80	2.9		2437962	13.1	4.1
	2436968	2.69	2.2		2437972	1.13	3.3
	2436973	0.98	2.2	2437965	2437999	2.80	3.9
	2436944	8.77	1.2		2437964	0.56	2.0
	2436958	5.51	4.3	2437972	2437948	0.59	2.7
	2436932	0.74	2.3		2437987	2.44	3.6
2437040	2437028	4.21	0.6		2437962	11.6	1.1
	2437022	0.63	1.5		2437957	0.89	3.3
2437103	2437059	1.28	4.2	2437976	2437937	3.59	3.8
	2437041	0.60	4.8		2437931	1.28	4.3
2437171	2437220	0.85	4.6		2437932	1.87	4.3
2437240	2437220	5.90	0.9		2437926	0.58	4.6
	2437184	0.67	3.5		2437964	3.54	4.5
2437270	2437315	0.92	3.3	2437987	2437996	1.26	4.7
	2437323	5.85	3.7		2437962	4.76	3.2
	2437299	6.47	2.2	2438038	2438078	2.81	4.0
	2437348	1.92	5.0	2438051	2438073	0.79	2.2
	2437234	5.18	3.1		2438032	0.65	5.0
	2437257	3.26	2.5	2569945	2569926	5.14	2.3
	2437267	2.73	2.6		2569891	1.07	5.0
2437325	2437402	1.87	4.4		2569925	0.85	2.7
	2437313	7.21	4.2	2570094	2570091	2.15	3.3
	2437329	0.64	3.7		2570079	2.34	1.2
	2437255	0.56	4.9	2570172	2570182	0.63	2.7
2437353	2437317	0.67	4.8		2570131	0.78	4.9
2437394	2437331	0.65	4.1	2570214	2570226	2.05	1.5
2437402	2437410	0.67	1.4	2570244	2570277	0.94	3.7
	2437405	0.97	4.8	2570384	2570400	4.84	3.7
	2437325	0.54	4.4		2570370	21.4	3.5
2437488	2437437	1.26	4.5	2570518	2570524	1.08	3.7
	2437429	3.06	4.7		2570536	2.76	3.5
2437496	2437487	0.59	4.9				

^aOnly targets for which we detect oscillations are listed.

^bFlux ratio between potential blend and target.

the blending star is very similar to that of the target would the measured $\Delta\nu$ and ν_{\max} be affected. In addition, variability from a blending star, such as a binary companion, could dominate and hence get detected instead of that from the target.

We made similar plots replacing K band with J , H , and V to see if they showed consistent results. The last is shown in Figure 7 (panel B). The V band clearly shows larger scatter than the infrared bands due to its stronger sensitivity to differential interstellar reddening and the slight temperature difference between clump and red-giant-branch stars of the same mean density. The bending of the main trend (dashed lines) is due to strong blanketing affecting the V band measurements for the cooler stars (see Figure 3 in Garnavich et al.

TABLE 5
POTENTIAL BLENDS FOR NGC 6819 TARGETS.

Target ID ^a (KIC)	Blend (KIC)	$\frac{\text{Flux}_B}{\text{Flux}_T}$ ^b	Sep (pix)	Target ID ^a (KIC)	Blend (KIC)	$\frac{\text{Flux}_B}{\text{Flux}_T}$ ^b	Sep (pix)
5024297	5024272	4.58	4.6	5024601	5024582	0.83	2.9
	5024312	0.56	2.4		5112741	1.07	3.4
5024312	5024297	1.78	2.4		5112751	0.83	4.3
	5024349	3.83	4.9	5111940	5111932	2.00	2.4
5024405	5024410	2.55	3.2	5112467	5112445	0.69	2.4
5024414	5024410	1.04	2.9		5112478	0.80	2.4
	5024369	0.81	4.8		5112491	1.04	2.9
5024456	5024470	2.51	3.2	5112491	5112467	0.97	2.9
5024512	5024517	1.38	3.5		5112478	0.78	3.3
	5024511	2.66	3.0	5112734	5024582	1.03	3.8
5024517	5024511	1.93	0.9		5112741	1.33	2.4
	5024512	0.73	3.5		5112751	1.04	3.2
5024582	5024601	1.21	2.9	5112751	5024582	1.00	4.5
	5112734	0.97	3.8		5024601	1.21	4.3
	5112741	1.29	2.8		5112734	0.97	3.2
	5112751	1.00	4.5		5112741	1.29	1.7
5024583	5024584	4.99	1.0	5112938	5112932	0.68	2.9

^aOnly targets for which we detect oscillations are listed.

^bFlux ratio between potential blend and target.

1994). Interestingly, this comparison revealed that for one star, KIC5024517, the V and H band measurements aligned with the expected trend of cluster members, while in K and J bands the star was an outlier (see arrow). In addition, there are indications in the power spectrum of excess power from two oscillating stars. The excess located at the highest frequency (picked up by the time series analysis pipelines) is compatible with the star being a cluster member if we use the V and H band measurements, while the low frequency excess is in agreement with the K and J band measurements. This strongly suggests that blending (Tables 2 and 5) has affected the standard photometry as well as the *Kepler* light curve.

6.1. Estimating $\Delta\nu$ and ν_{\max}

In the next step, we will estimate the expected $\Delta\nu$ and ν_{\max} from solar scaling (Eqs. 1 and 2), and compare them directly with the observations to make inference on cluster membership. We do note that because these two parameters are so strongly correlated (Stello et al. 2009; Hekker et al. 2009; Mosser et al. 2010), using both adds little extra information other than redundancy for the purpose of determining membership.

To estimate the expected $\Delta\nu$ and ν_{\max} we converted the apparent magnitude into luminosity, using the cluster distances by Basu et al. (2011). For NGC 6811, which was not studied by Basu et al. (2011), we adopted a distance modulus of 10.3 mag found by visual isochrone fitting. The contribution to the spread in apparent magnitude from the intrinsic depth of the clusters is similar to that from the photometric uncertainty, and is ignored in the following. We adopted average cluster reddenings of $E(B - V) = 0.16$ mag (NGC 6791, Brogaard et al. (2011)), $E(B - V) = 0.14$ mag (NGC 6819, Bragaglia et al. (2001)), and $E(B - V) = 0.16$ mag (NGC 6811, Webda database). Bolometric corrections were performed using the calibrations by Bessell & Wood (1984) and Flower (1996).

The scatter in the mass of these red-giant-branch stars can be assumed to be low (less than 1% along a standard isochrone, e.g. Marigo et al. (2008)). We therefore adopted

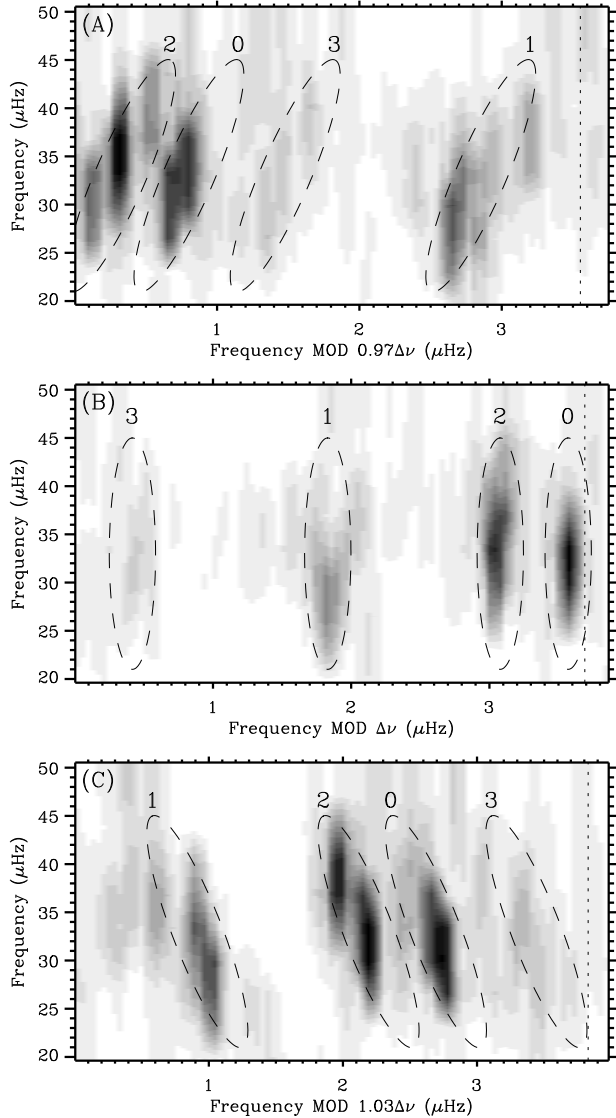


FIG. 5.— Échelle diagrams of the power spectrum of KIC2436824. The power spectrum was smoothed for better visual impression. Ellipses indicate the four ridges formed by oscillation modes of spherical degrees $l = 0-3$. The dotted lines mark the expected position of the radial ($l = 0$) modes (see text). Each panel shows the échelle for slightly different choices of the segment width used to divide the power spectrum. Panel B shows the best choice of $\Delta\nu$.

the average red giant mass from Basu et al. (2011) for NGC 6791 and NGC 6819. It should be noted that the assumed common mass might result in a systematic overestimation of the expected $\Delta\nu$ for the red clump stars – not included in the study by Basu et al. (2011) – if they have experienced significant mass loss compared to the red-giant-branch stars (Miglio et al. 2011). We indicate in Table 1 (column-5), Table 2 (column-6), and Table 3 (column-6) which stars are clump stars inferred from the color-magnitude diagram (Figure 2). For NGC 6811, we used an average mass of $2.35 M_{\odot}$ derived from $\Delta\nu$, ν_{\max} , and T_{eff} by combining Equations 1 and 2 (Kallinger et al. 2010b) similar to what was done by Hekker et al. (2011). Finally, we emphasize that the absolute values adopted for the average cluster properties are of less importance since we are looking only to distinguish stars that deviate from the average trend. Hence, it is important to

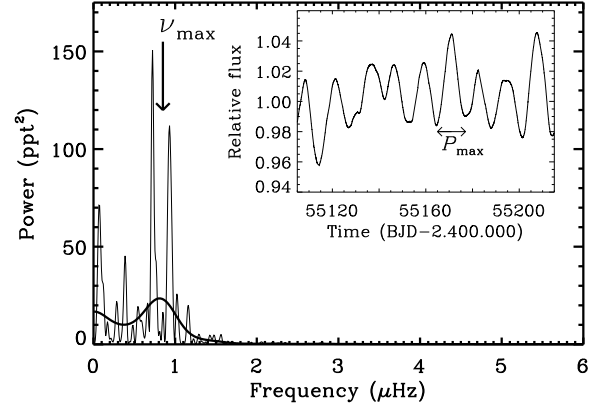


FIG. 6.— Power spectrum and part of light curve (inset) of one of the long period stars where $\Delta\nu$ could not be reliably determined (KIC2437171). The thick curve shows the spectrum convolved with a Gaussian function of FWHM $\sim 0.4 \mu\text{Hz}$. The frequency of maximum power, ν_{\max} , and corresponding dominant periodicity in the light curve are indicated with arrows.

take into account the relative T_{eff} and bolometric corrections of each star.

To obtain T_{eff} we transformed the $V - K$ color index using the calibrations by Ramírez & Meléndez (2005). We estimate the uncertainty in T_{eff} to be ~ 100 K, which includes contributions from the photometry, color-temperature calibration, and reddening (Hekker et al. see 2011 for further details). As a double check we compared our T_{eff} with those derived from $B - V$. The results are shown in Figure 8. The offset seen for NGC 6819 shows a slight dependency with color and is most likely due to calibration errors in the standard photometry.

The $V - K$ index is generally the better temperature proxy for cool red giants, it is less sensitive to metallicity, and its temperature calibration show lower scatter than for $B - V$. We therefore choose $V - K$. The two outliers, KIC2437171 and KIC2438421, are much cooler than they appear in $B - V$ (Garnavich et al. 1994), supporting that $V - K$ is the preferred color index. However, for KIC5024517 – the outlier in NGC 6819 – we recall that the K -band measurement is probably affected by blending (Figure 7), suggesting $V - K$ might not be the best temperature indicator in this case.

6.2. Results on the observed-to-expected ratio

The observed-to-expected ratios for $\Delta\nu$ and ν_{\max} are shown in Figure 9. The expected ratio is 1.0, with an uncertainty slightly below 10% ($1-\sigma$ region marked in gray), which is dominated by the uncertainty in T_{eff} . The size of the uncertainty underpins that ignoring the expected spread in mass of $\lesssim 1\%$ is sound. For our purpose the absolute value of the average ratio is not important but rather the deviation of single stars from the ensemble. However, it turns out that the majority of stars fall close to 1.0, which shows that any possible systematic errors in the expected (scaled) $\Delta\nu$ and ν_{\max} , caused by offsets in the calibration of the scaling relations or inaccurate adopted cluster parameters, have cancelled out. Apart from a few clear outliers we see generally little scatter, which indicates that blending is less of an issue than suggested by the large number of potential blends, particularly for NGC 6791 (Table 1, column-4). We note that we did not find any general trends between on the one hand stellar brightness or color and the other hand the deviation of $\Delta\nu$ and ν_{\max} from the clus-

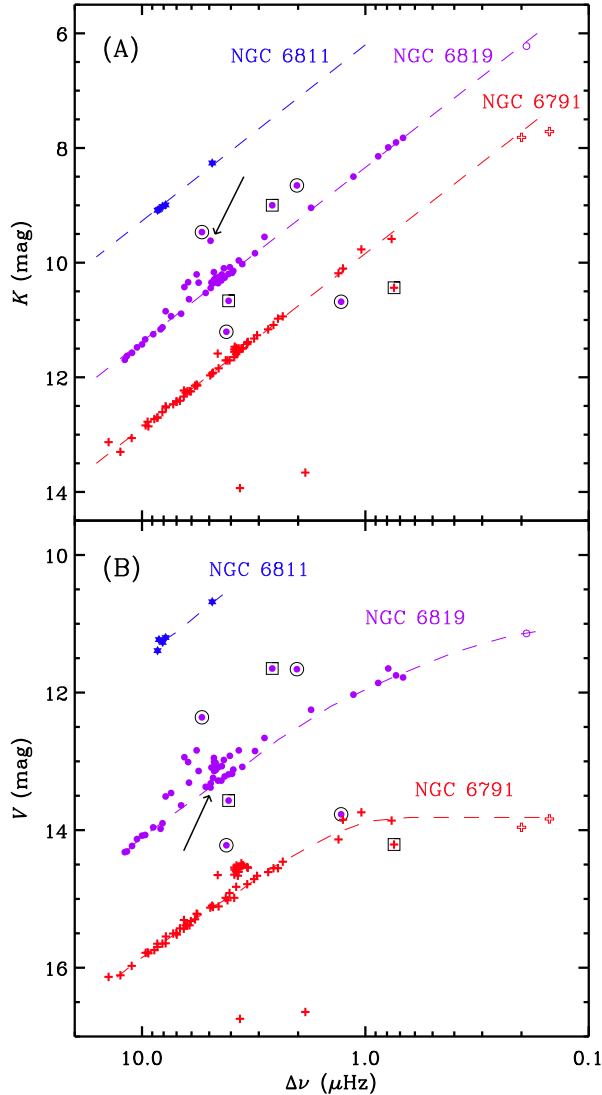


FIG. 7.— Apparent magnitude versus large separation for NGC 6811 (blue stars), NGC 6819 (purple dots), and NGC 6791 (red pluses). Open symbols show preliminary results for stars with very low $\Delta\nu$. Axes are oriented to make the plots resemble a color-magnitude diagram. Dashed fiducial lines are shown to guide the eye. Arrow marks KIC5024517 (see text). Non-members from Stello et al. (2010) are encircled. Newly established non-members (this work) are bracketed by squares (see Sect. 6.2).

ter average. Nor did we detect a difference in the observed-to-expected ratios between stars on the red giant branch and the red clump; hence supporting that any possible mass loss, which is expected to occur predominantly near the tip of the red giant branch, is insignificant compared to the uncertainty in the ratios plotted in Fig. 9. However, stars that do clearly deviate need to be carefully assessed before we draw any conclusions about their cluster membership. We will discuss each cluster in turn.

In NGC 6791 there are three outliers in $\Delta\nu$ (KIC2297793, 2436954, 2437851) and an additional borderline case in ν_{\max} (KIC2438421). The latter is one of the stars with very low $\Delta\nu$ and ν_{\max} for which accurate uncertainties were difficult to determine and we therefore do not make a final conclusion on its membership. Of the others, KIC2436954 and 2437851 are the two faintest stars ($V \simeq 16.1$, $Kp \simeq 16.4$)

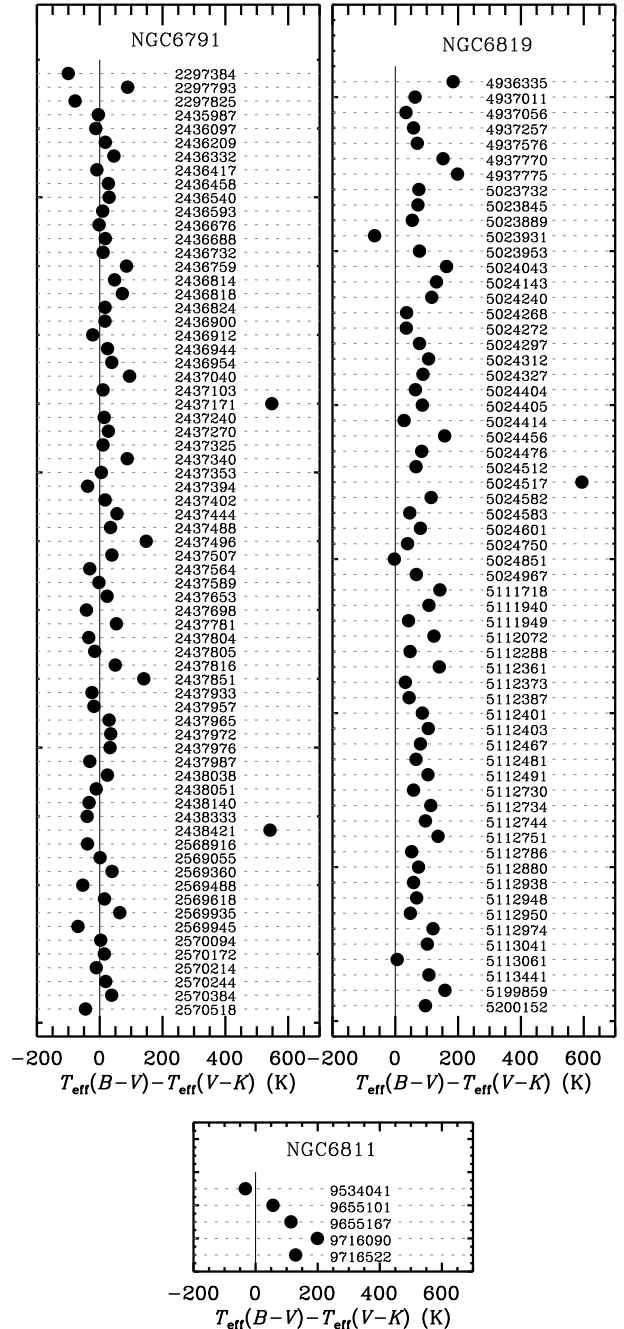


FIG. 8.— Difference between temperatures derived from the $B - V$ and $V - K$ color indices.

for which oscillations have been detected. The former shows strong evidence of blending, while the latter is potentially blended. This leaves KIC2297793 as the only star where we can not explain the results as potentially due to blending. The fast stage of evolution of this very luminous star (upper red giant or asymptotic giant branch assuming it is a cluster member) means that a potential binary companion would presumably be much fainter, making it unlikely that the companion affects our measurements significantly (both seismic as well as the standard photometry). We therefore conclude the most likely explanation is that the star is not a cluster member. For some of the targets we have membership probabilities from

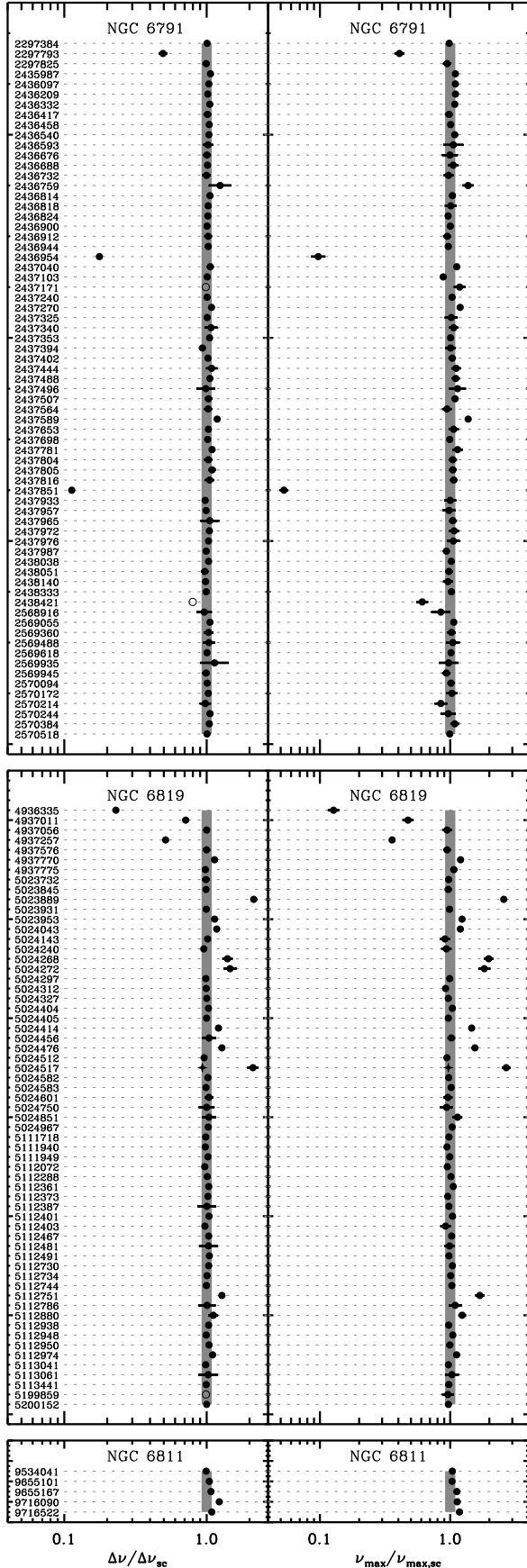


FIG. 9.— Ratio between measured and solar-scaled $\Delta\nu$ (left) and ν_{\max} (right) for targets in NGC 6791 (top), NGC 6819 (middle), and NGC 6811 (bottom). The $1\text{-}\sigma$ region of the expected ratio is shown in gray. Open symbols show preliminary results for stars with very low $\Delta\nu$. Star symbols show results using the $B - V$ temperature (see text for details).

radial velocity (Meibom & Platais, priv. comm. (2010) and Garnavich et al. (1994)), and from both radial velocity and metallicity (Worthey & Jowett 2003; Origlia et al. 2006; Carraro et al. 2006; Gratton et al. 2006), which we list in Table 1 (column-6–8), while column-9 lists our seismic membership results. Our results on KIC2297793 reaffirm that of Garnavich et al. (1994) who’s ambiguous ‘no?’ designation was chosen because the star’s radial velocity was significantly different from the cluster average despite moving in the same direction as the cluster as opposed to the bulk of the field. Finally, it is noticeable that quite a few seismic members – all initially selected as photometric members – are assigned low probability membership from the radial velocity survey by (Meibom & Platais). We speculate that this could be due to binary companions, which we will address using seismology in a forthcoming paper.

NGC 6819 shows a few more outliers than NGC 6791 despite the stars being brighter and less affected by blending (compare Tables 4 and 5). Our results confirm all four seismic non-members identified by Stello et al. (2010) KIC4936335, 4937257, 5023889, and 5024272. In addition, we can identify two new seismic non-members, KIC4937011 and 5024268. All other apparently discrepant stars could be explained by potential blending or binarity (KIC5024414, 5024476, 5024517, and 5112751) affecting both the seismic measurements and the temperature estimates (spectroscopic binaries are listed in Table 2 column-7). In fact, adopting the temperature from $B - V$ for KIC5024517 makes it agree quite well (star symbol). We see the opposite in KIC5023931, which is a known binary where the $V - K$ temperature and the detected oscillations agree with membership, while it would appear as a non-member if we adopt the $B - V$ temperature. For comparison we list membership probabilities from radial velocity, and proper motion in Table 2 (column-8 and 9), as well as photometric membership alongside the identified seismic membership (column-10 and 11). In four cases stars appear to be both seismic and photometric non-members. Three stars (KIC5112880, 5113041, and 5113441) have very low proper motion probability contradicting the results from radial velocity, photometry, and seismology.

Finally, all five stars selected in NGC 6811 show seismic signals that agree with them being cluster members (Table 3, column-12). Our results agree well with those inferred from radial velocity measurements (column-7 and 8), proper motion (column-9 and 10), and photometric membership (column-11).

7. DISCUSSION AND CONCLUSION

We have demonstrated that cluster membership determined from seismology show advantages over more orthodox methods, and hence offers important complementary information to that of kinematic and photometric measurements. In our asteroseismic investigation we implicitly assumed a standard evolution history for the cluster stars when estimating the seismic parameters. Any exotic stars, such as remnants of strong dynamic interactions, would therefore appear as non-members under this assumption. While a kinematic study does not assume a standard stellar evolution, it can assign spurious field stars as members and vice versa if the space velocity of the cluster is not clearly distinct from that of the field. The asteroseismic determination, however, is insensitive to that, as it essentially separates non-members from members by revealing stars that are at a different distance than the ensemble mean.

From almost a year of *Kepler* data, we were able to measure global seismic properties of over a hundred red giant stars in three open clusters allowing inference to be made on the cluster membership of each star. Among our list, comprising likely members determined from photometric and kinematic surveys, we found three new non-members and confirmed the four previously identified seismic non-members by Stello et al. (2010). We found more seismic non-members in NGC 6819 despite this cluster having fewer members than NGC 6791. This could indicate issues with obtaining a clean sample of members purely from the kinematic properties of NGC 6819. However, we note that a probably significant contribution to the difference in number of identified non-members in these two clusters comes from the different selection criteria adopted for each cluster.

Finally, we highlighted that the presence of binary stars and blends needs careful investigation to avoid misinterpretation of the seismic results as well as the auxiliary standard photometry. In some cases the light curves revealed seismic signal from more than one star, which could be used to identify and to some extent disentangle signals from blends and binaries.

Future *Kepler* data of the so-called cluster super stamps will

give access to most stars in NGC 6791 and NGC 6819, providing more comprehensive assessment of the effects from blending, and enable us to make unbiased selections of the cluster stars, which will further extend the asteroseismic analyses of these clusters. In addition, we will get short cadence data (1-minute sampling) of selected stars in NGC 6819 which will allow us to probe the interiors of the less evolved turn-off and subgiant stars.

Funding for this Discovery mission is provided by NASA's Science Mission Directorate. The authors would like to thank the entire *Kepler* team without whom this investigation would not have been possible. DS acknowledges support from the Australian Research Council. This project has been supported by the 'Lendület' program of the Hungarian Academy of Sciences and the Hungarian OTKA grant K83790 and MB08C 81013. SH acknowledges financial support from the UK Science and Technology Facilities Council (STFC). KB acknowledges financial support from the Carlsberg Foundation. NCAR is supported by the National Science Foundation. RS thanks the support of the János Bolyai Research Scholarship.

REFERENCES

- Basu, S., et al. 2011, *ApJ*, 729, L10
 Bessell, M. S., & Wood, P. R. 1984, *PASP*, 96, 247
 Bragaglia, A., et al. 2001, *AJ*, 121, 327
 Brogaard, K., Bruntt, H., Grundahl, F., Clausen, J. V., Frandsen, S., Vandenberg, D. A., & Bedin, L. R. 2011, *A&A*, 525, A2
 Brown, T. M., Gilliland, R. L., Noyes, R. W., & Ramsey, L. W. 1991, *ApJ*, 368, 599
 Carraro, G., Villanova, S., Demarque, P., McSwain, M. V., Piotto, G., & Bedin, L. R. 2006, *ApJ*, 643, 1151
 Christensen-Dalsgaard, J. 2004, *Sol. Phys.*, 220, 137
 Dias, W. S., Lépine, J. R. D., & Alessi, B. S. 2002, *A&A*, 388, 168
 Flower, P. J. 1996, *ApJ*, 469, 355
 Garcia, R. A., et al. 2011, *MNRAS*, 414, 6
 Garnavich, P. M., Vandenberg, D. A., Zurek, D. R., & Hesser, J. E. 1994, *AJ*, 107, 1097
 Gratton, R., Bragaglia, A., Carretta, E., & Tosi, M. 2006, *ApJ*, 642, 462
 Hekker, S., et al. 2009, *A&A*, 506, 465
 —. 2010, *MNRAS*, 402, 2049
 —. 2011, *A&A*, 530, 100
 Hole, K. T., Geller, A. M., Mathieu, R. D., Platais, I., Meibom, S., & Latham, D. W. 2009, *AJ*, 138, 159
 Huber, D., Stello, D., Bedding, T. R., Chaplin, W. J., Arentoft, T., Quirion, P., & Kjeldsen, H. 2009, *Communications in Asteroseismology*, 160, 74
 Huber, D., et al. 2010, *ApJ*, 723, 1607
 Jenkins, J. M., et al. 2010a, *ApJ*, 713, L120
 —. 2010b, *ApJ*, 713, L87
 Kallinger, T., et al. 2010a, *A&A*, 522, 1
 —. 2010b, *A&A*, 509, 77
 Kjeldsen, H., & Bedding, T. R. 1995, *A&A*, 293, 87
 Koch, D. G., et al. 2010, *ApJ*, 713, L79
 Marigo, P., Girardi, L., Bressan, A., Groenewegen, M. A. T., Silva, L., & Granato, G. L. 2008, *A&A*, 482, 883
 Mathur, S., et al. 2010, *A&A*, 511, 46
 Mermilliod, J., & Mayor, M. 1990, *A&A*, 237, 61
 Miglio et al. 2011, in prep.
 Mosser, B., & Appourchaux, T. 2009, *A&A*, 508, 877
 Mosser, B., et al. 2010, *A&A*, 517, 22
 —. 2011, *A&A*, 525, L9
 Origlia, L., Valenti, E., Rich, R. M., & Ferraro, F. R. 2006, *ApJ*, 646, 499
 Pietrinferni, A., Cassisi, S., Salaris, M., & Castelli, F. 2004, *ApJ*, 612, 168
 Ramírez, I., & Meléndez, J. 2005, *ApJ*, 626, 465
 Sanders, W. L. 1971, *A&A*, 15, 368
 —. 1972, *A&A*, 19, 155
 Skrutskie, M. F., et al. 2006, *AJ*, 131, 1163
 Stello, D., Bruntt, H., Preston, H., & Buzasi, D. 2008, *ApJ*, 674, L53
 Stello, D., Chaplin, W. J., Basu, S., Elsworth, Y., & Bedding, T. R. 2009, *MNRAS*, 400, L80
 Stello, D., et al. 2010, *ApJ*, 713, L182
 Stello et al. 2011, *ApJ* in press (arXiv:1107.0490)
 Stetson, P. B., Bruntt, H., & Grundahl, F. 2003, *PASP*, 115, 413
 Ulrich, R. K. 1986, *ApJ*, 306, L37
 White et al. 2011, *ApJ* submitted
 Worthey, G., & Jowett, K. J. 2003, *PASP*, 115, 96